

Evaluating the use of Carpal bones for the determination of skeletal maturity for infants.

Steve A. Adeshina
steve.adeshina@postgrad.manchester.ac.uk

Timothy F. Cootes
t.cootes@manchester.ac.uk

Judith E. Adams
judith.adams@manchester.ac.uk

Imaging Science and Biomedical
Engineering,
School of Cancer and Enabling
Sciences,
The University of Manchester,
Manchester, UK.

Abstract

We compare the utility of models of the structure of carpal bones in the hand for predicting skeletal maturity in infants (0 -7 yrs). Skeletal maturity assessment is important for diagnosing and monitoring growth disorders. Statistical models of bone shape and appearance have been shown to be useful for estimating skeletal maturity. In this work we investigate the effect of the choice of models of different carpal bones' structure on prediction performance. By analysing the performance on a dataset of 294 digitized radiographs of normal infants we show that a simple texture based appearance model of the carpal region produces the best results. Our results show a mean absolute error of (0.42, 0.53) years, for female and male, from such a texture based model.

1 Introduction

Skeletal maturity plays an important role in the diagnosis of growth and endocrine disorders. The two main methods examine the morphology of the bones and the joints of the non-dominant hand in a radiograph. A significant difference between the bone age and the actual age of a child is an indication of growth abnormalities. The predominant methods in clinical practice are those of Greulich and Pyle(GP) [1] and Tanner and Whitehouse(TW2/3) [2].

There have been many attempts to automate the bone age assessment procedure. These range from classical image analysis methods [3], machine learning techniques and model based methods [4]. Thodberg *et al.* [5] recently showed how Active Appearance Models [6] can be used to determine skeletal maturity. However the estimation was limited to 2 - 17 years and excluded the use of carpal bones.

The key issue here is that the most critical years during which corrective procedures can easily be carried out are excluded in maturity estimation. The reason may be due to the lack of availability of images and the poor radiograph image quality at this early age. The Carpal bones, which are the most useful at this stage, are either in cartilage form or are just appearing as a dot as shown in Figure 1. Their order of appearance is not consistent. Zhang *et al.* [7] used classical image processing techniques and fuzzy classification to estimate bone

age from the Hamate and Capitate (see Figure 1). We differ in our approach from Zhang *et al.* as we use statistical models of appearance to evaluate the utility of the carpal bones from ages 0 -7 years. This work is intended to complement our earlier work [10] where we evaluated several structures in estimating skeletal maturity, but the work was limited to ages above 5 years. It will also complement the work of Thodberg *et al.* [8], who estimated age from 2 years without the use of carpal bones.

The main problem is that of correspondence which results from inconsistent appearance of the component carpal bones as illustrated in Figure 1. In our approach we built several variants of statistical models of appearance, the parameters of which were used in a linear regressor to predict the 'common' (race normalized) bone age of the child.

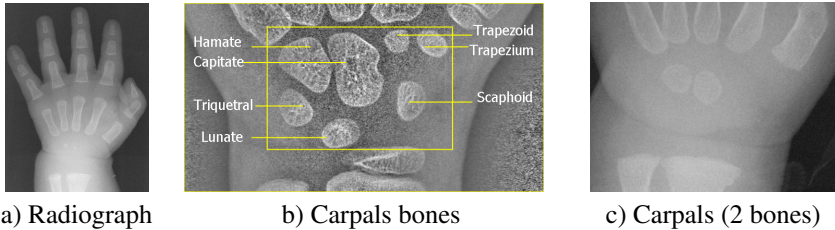


Figure 1: a) Example of a hand radiograph of a child with no bones, b) Carpal bones labeled and c) carpal region with two bones.

2 Methods

2.1 Data Set

We have used a publicly available database of radiographs of the non-dominant hand of normally developing children from Ipilab laboratories¹. We used a subset of 294 images representing ages from 0 -7 years. The dataset are of children from 4 ethnic groups (Caucasians, Asians, African Americans and Hispanics). The data also comes with two independent expert ratings who were blinded to the chronological age and the ethnicity of the children at the time of reading.

In studying the structures of the carpal bones, we regard the expert average of the bone age as 'common' bone age.

2.2 Construction of Statistical Appearance Models

Statistical appearance models (SAM) [10] were generated by combining a model of shape variation with a model of texture variation. Each radiograph was manually annotated with points around important structures. Statistical models of shape and texture (intensities in the reference frame) were constructed by applying Principal Component Analysis (PCA) to the resulting annotations, leading to linear models of the form

$$\mathbf{x} = \bar{\mathbf{x}} + \mathbf{P}_s \mathbf{b}_s \quad \mathbf{g} = \bar{\mathbf{g}} + \mathbf{P}_g \mathbf{b}_g \quad (1)$$

where $\bar{\mathbf{x}}$ is the mean shape, $\bar{\mathbf{g}}$ is the mean texture, $\mathbf{P}_s, \mathbf{P}_g$ are the main modes of shape and texture variation and $\mathbf{b}_s, \mathbf{b}_g$ are the shape and texture model parameter vectors. Combining

¹<http://www.ipilab.org/BAWeb/>

the shape and texture models gives a combined appearance model of the form

$$\mathbf{x} = \bar{\mathbf{x}} + \mathbf{Q}_s \mathbf{c} \quad \mathbf{g} = \bar{\mathbf{g}} + \mathbf{Q}_g \mathbf{c} \quad (2)$$

where \mathbf{Q}_s , \mathbf{Q}_g are matrices describing the modes of variation derived from the training set and \mathbf{c} is a combined vector of appearance parameters controlling both shape and texture.

2.3 Groupwise registration

The manual annotation uses only a few points for each local bone complex model, so does not represent details of the bone shape. To improve the density of the correspondences we applied a ‘groupwise’ non-rigid registration algorithm, similar to that in [9], initialised with the manual points. For each structure we defined a dense triangulated mesh on one image, then used the manual annotation to propagate this to the other images using thin-plate spline interpolation. We then estimated the mean shape and texture and applied a non-rigid registration approach to improve the correspondence between each image and the mean. The process is repeated until convergence, leading to an accurate, dense correspondence across the set. Models of shape, texture and appearance were then constructed from the resulting points.

2.4 Estimation of skeletal maturity

Given the appearance models we can compute shape, texture and appearance parameter vectors for each structure on each image.

We use classical linear regression of the form, $A = \mathbf{w}^T \mathbf{p} + A_0$, where A is the predicted age, \mathbf{w} is a vector of weights, \mathbf{p} is the parameter vector and A_0 is a constant. In the following we describe experiments comparing the performance of different models of the carpal bones.

3 Experiments

We built several carpal bones’ models as in Figure 3 from annotations shown in Figure 2. We describe the texture model and each of the appearance models (AM) as follows:

- a) A texture model built from 17 points around the carpal region (Figures 2a and 3a).
- b) An AM of all carpal bones built from points around each of 7 bones (Figures 2b and 3b).
- c) An AM built from points around the carpal region and around 2 consistent bones (Figures 2c and 3c).
- d) An AM built from points around 4 bones with registration (Figures 2d and 3d).
- e) An AM built from points around 5 bones with registration (Figures 2e and 3e).
- f) An AM built from points around 2 consistent bones with registration (Figures 2f and 3f).
- g) A group AM built from images with 2 bones from the dataset. Groups of 2,4-6 and 7 bones were also built (Figures 2g and 3g).
- h) An AM built from single Capitate bone with registration (Figures 2h and 3h).
- i) An AM built from single Hamate bone with registration (Figures not shown. Results in Table 1, item i).

Images of males and females were pooled to create the models.

For each model we computed the shape, texture and appearance parameters for every image. We then evaluated the utility of linear age prediction models using a Leave-One-Out (LOO) paradigm. We trained linear regressors to predict age on all but one image, then tested

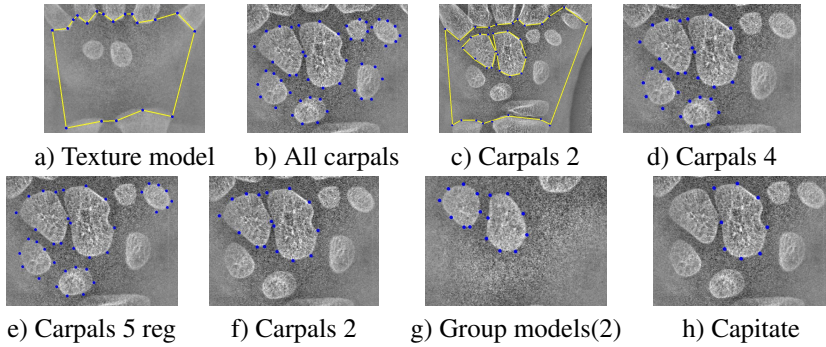


Figure 2: Annotation for different models. Legends corresponds to Table 1

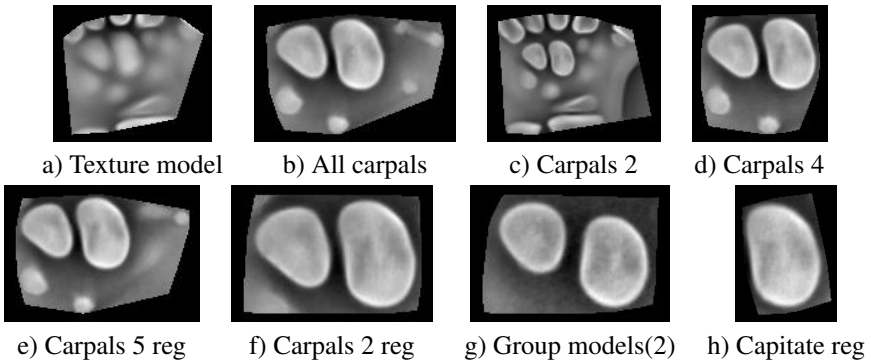


Figure 3: Carpals models. Legends corresponds to Table 1

the prediction on the left-out image. Since male and female children are known to develop at different rates, different regressor models were used for the male and the female sets. We evaluated performance using the mean absolute error between prediction and the average of the expert readings, which we refer to as ‘common’ bone age.

4 Discussion and Conclusion

The result in tables 1 show that the best performance was obtained from the texture based model (a). It is the simplest with 17 points around the carpal region. This show that it is possible to estimate the changes in shape and the appearance of bones in the carpal region and thereby estimate skeletal maturity even in the absence of individual bones’ correspondence. The texture model solved the problems of lack of correspondence in the carpal region in early ages and can be applied in other applications.

The texture model result of mean absolute errors of 0.42, 0.53 years in table 1 compares favourably with other figures from the literature [9], [8] and [11]. This is especially so when the inter- and intra- rater variability associated with the expert reading with which we trained the regressor is considered. We believe this method provides an effective way of estimating skeletal maturity for often neglected infants. In future we hope to extract the Carpals region of interest automatically.

	Female			Male		
	Shape	Tex.	App.	Shape	Tex.	App.
a	<i>na</i>	0.42 ±0.03	<i>na</i>	<i>na</i>	0.53 ±0.04	<i>na</i>
b	0.44±0.03	0.47±0.04	0.49±0.03	0.65±0.04	0.83±0.05	0.71±0.04
c	0.49±0.03	0.44±0.03	0.52 ±0.03	0.54±0.04	0.60±0.04	0.61±0.04
d	0.50±0.03	0.62±0.05	0.49±0.03	0.64±0.05	0.70±0.05	0.64±0.05
e	0.45±0.03	0.52±0.04	0.48±0.03	0.66±0.04	0.72±0.05	0.74±0.05
f	0.47±0.03	0.54±0.04	0.54±0.04	0.65±0.05	0.78±0.05	0.70±0.05
g	0.44 ±0.03	0.49±0.04	0.46±0.05	0.68 ±0.04	0.80±0.05	0.61±0.05
h	0.66±0.05	0.73±0.05	0.69±0.06	0.94±0.07	1.02±0.07	1.11±0.1
i	0.58±0.05	0.74±0.05	0.61±0.05	0.84±0.06	0.95±0.06	0.82±0.06

Table 1: Average performance various carpal based models - Mean absolute prediction error for female and male (years). Letters correspond to description in Section 3 and models shown in Figure 3

References

- [1] Steve A. Adeshina, Timothy F. Cootes, and Judith Adams. Evaluating different structures for predicting skeletal maturity using statistical appearance models. In *Proc. MIUA*, 2009.
- [2] T. F. Cootes, G. J. Edwards, and C. J. Taylor. Active appearance models. *IEEE Transactions on Pattern Analysis and Machine Intelligence*, 23(6):681–685, 2001.
- [3] T.F. Cootes, C.J. Twining, V.Petrović, R.Schestowitz, and C.J. Taylor. Groupwise construction of appearance models using piece-wise affine deformations. In *16th British Machine Vision Conference*, volume 2, pages 879–888, 2005.
- [4] W. W. Greulich and S. I. Pyle. *Radiographic Atlas of Skeletal Development of Hand Wrist*. Palo Alto, CA: Stanford Univ. Press, 1971.
- [5] M. Niemeijera, B. van Ginnekena, C.A. Maasa, F.J.A. Beek, and M.A. Viergevera. Assessing the skeletal age from a hand radiograph: automating the tanner-whitehouse method. In *Proceedings of SPIE – Volume 5032*, pages 1197–1205, May 2003.
- [6] E. Pietka, A. Gertych, S. Pospiech, Fei Cao, H. K. Huang, and V. Gilsanz. Computer-assisted bone age assessment: image preprocessing and epiphyseal/metaphyseal roi extraction. *IEEE Transactions on Medical Imaging*, 20(8):715–729, 2001.
- [7] J. M. Tanner, R. H. Whitehouse, W. A. Marshall, M. R. Healy, and H. Goldstein. *Skeletal Maturity and Prediction of Adult Height (TW2 Method)*. New York, NY: Academic, 1975.
- [8] H.H. Thodberg, S. Kreiborg, A. Juul, and K.D Pedersen. The bonexpert method for automated determination of skeletal maturity. *Medical Imaging, IEEE Transactions on*, 1(1309):52–66, 2009.
- [9] A. Zhang, A. Gertych, and B. Liu. Automatic bone age assessment for young children from newborn to 7-year-old using carpal bones. *Computerized Medical Imaging and Graphics*, 31:299–310, 2007.